Available online at www.sciencedirect.com
SCIENCE DIRECT®
European Journal of Pharmacology 457 (2002) 19–27
www.elsevier.com/locate/ejphar

Inhibitory effect of the class III antiarrhythmic drug nifekalant on HERG channels: mode of action

Shunichi Kushida[a,b], Takehiko Ogura[a], Issei Komuro[b], Haruaki Nakaya[a,*]

[a] *Department of Pharmacology, Chiba University Graduate School of Medicine, Inohana 1-8-1, Chuo, Chiba 260-8670, Japan*
[b] *Department of Cardiovascular Science and Medicine, Chiba University Graduate School of Medicine, Inohana 1-8-1, Chuo, Chiba 260-8670, Japan*

Received 3 June 2002; received in revised form 23 October 2002; accepted 29 October 2002

Abstract

Nifekalant is a class III antiarrhythmic drug that has been shown to be effective against ventricular tachyarrhythmias in experimental animals and humans. We examined the detailed electrophysiological effects of nifekalant on human-ether-a-go-go-related gene (HERG) channels expressed in *Xenopus* oocytes. Nifekalant inhibited the HERG current in a concentration-dependent manner with an IC_{50} value of 7.9 μM although the drug did not inhibit the minK current in *Xenopus* oocytes, suggesting selective inhibition of the rapid component of the delayed rectifier K^+ current (I_{Kr}) in cardiomyocytes. Nifekalant showed a higher binding affinity for the open state than for the inactive state of HERG channels. Nifekalant inhibited HERG channels in a frequency-dependent manner. The onset of the blockade was rapid but the recovery from the block was slow. Nifekalant modified the voltage dependence and kinetics of HERG channel gating. Thus, nifekalant inhibits HERG channels in a voltage-dependent and frequency-dependent manner, and the inhibitory effect may underlie the clinical efficacy of the drug against ventricular tachyarrhythmias.

Keywords: Antiarrhythmic agent; Ion channel; Voltage dependence; Frequency dependence

1. Introduction

Sudden cardiac death is primarily the result of lethal ventricular arrhythmias. Class III antiarrhythmic drugs are assumed to control life-threatening ventricular arrhythmias by retarding repolarization mainly through inhibition of the rapidly activating component of the delayed rectifier potassium current (I_{Kr}) (Mason, 1993; Waldo et al., 1995). Class III antiarrhythmic agents commonly possess an unfavorable electophysiological property, namely, they lengthen action potential duration in a reverse use-dependent manner. Moreover, their action potential duration-prolonging effects become more pronounced at low vs. high stimulation frequencies, which may cause a proarrhythmic effect during bradycardia (Hondeghem and Snyders, 1990).

Nifekalant hydrochloride is a novel class III antiarrhythmic agent that has recently become available for clinical use (Nakaya and Uemura, 1998). It differs from most methylsulfonamide class III antiarrhythmic agents (e.g., sotalol, E-4031(*N*-[4-[[1-[2-(6-methyl-2-pyridinyl)ethyl]-4-piperidinyl]carbonyl]phenyl]methanesulfonamide dihydrochloride dehydrate), dofetilide) in having a nitro group rather than a methylsulfonamide group in the *p*-position of the benzene ring. The drug prolongs the action potential duration mainly by blocking I_K, especially its rapid component (I_{Kr}) (Nakaya and Uemura, 1998). This agent was also found to have an inhibitory effect on various K^+ currents, including the transient outward K^+ current (I_{to}) (Nakaya et al., 1993; Cheng et al., 1996), the ATP-sensitive K^+ current ($I_{K.ATP}$) (Martin et al., 1995), the muscarinic acetylcholine receptor-operated K^+ current ($I_{K.ACh}$) (Mori et al., 1995) and the inward rectifier K^+ current (I_{K1}) (Nakaya et al., 1993; Sato et al., 1995), in high concentrations. The drug has been shown to be effective against various experimental arrhythmias (Kamiya et al., 1992; Friedrichs et al., 1994, 1995; Hashimoto et al., 1995; Kondoh et al., 1994). In experimental animals, nifekalant prevented the occurrence of ventricular tachyarrhythmias and improved electrical defibrillation efficacy (Kamiya et al., 1992; Murakawa et al.,

* Corresponding author. Tel.: +81-43-226-2050; fax: +81-43-226-2052.
E-mail address: nakaya@med.m.chiba-u.ac.jp (H. Nakaya).

0014-2999/02/$ - see front matter © 2002 Elsevier Science B.V. All rights reserved.
PII: S0014-2999(02)02666-3

1997). In clinical studies, nifekalant effectively suppressed malignant ventricular tachyarrhythmia associated with acute myocardial infarction in humans (Takenaka et al., 2001; Koizumi et al., 2001). It is acknowledged that human-ether-a-go-go-related gene (HERG) encodes the channel proteins through which I_{Kr} flows (Trudeau et al., 1995). In order to investigate the detailed pharmacological effect of nifekalant on I_{Kr}, we examined the effects of nifekalant on HERG channels expressed in *Xenopus* oocytes.

2. Methods

2.1. Oocyte preparation

The experiments were performed under the regulations of the Animal Research Committee of Chiba University Graduate School of Medicine. *Xenopus* oocytes were surgically removed from Xenopus laevis (Hamamatsu Seibutu, Hamamatu, Japan) under anesthesia in iced water. Stage V and VI *Xenopus* oocytes were enzymatically defolliculated by treatment with 2 mg/ml collagenase (type IA, Worthington Biochemical, Lakewood, NJ, USA) in Ca^{2+}-free OR-2 solution containing (mM) 82.5 NaCl, 1 KCl, 1 $MgCl_2$, 5 HEPES, pH 7.6, for 1.5 h and washed extensively with Ca^{2+}-free OR-2 solution without collagenase.

2.2. cRNA preparation and injection

Full-length HERG cDNA was obtained by polymerase chain reaction, using a human heart cDNA library (CLONTECH Laboratories, Palo Alto, CA, USA) as a template and was subcloned into an expression vector pcDNA 3.1 (Invitrogen, Carlsbad, CA, USA). cRNAs were prepared with the mMessage mMachine Kit (Ambion, Austin, TX, USA), using T7 RNA polymerase after linearization of the plasmid with *Eco*RI, according to the manufacturer's protocols.

The ooctytes were injected with 5 ng of HERG cRNA using a Drummond Nanoject microdispensor (Drummond Scientific, Broomhall, PA, USA) and incubated for 3–5 days at 18 °C in PS solution containing (mM) 96 NaCl, 2 KCl, 1.8 $CaCl_2$, 1 $MgCl_2$ and 5 HEPES, 2.5 pyruvate Na, 0.5 theophylline, supplemented with penicillin (100 U/ml) and streptomycin (100 μg/ml), pH 7.6, with NaOH.

2.3. Electrophysiological experiments

Membrane currents were recorded from oocytes with two-microelectrode voltage-clamp techniques, using an oocyte clamp amplifier (model OC-725C, Warner Instrument, Hamden, CT, USA). The microelectrodes were filled with 3 M KCl and had a resistance of 0.5–1.8 MΩ. Data acquisition was performed using pCLAMP software (version 5.7.1) and Digidata 1200 B (Axon Instrument, Foster City, CA, USA). Currents were recorded in ND 96 bath solution containing (mM) 96 NaCl, 2 KCl, 1.8 $CaCl_2$, 1 $MgCl_2$ and 5 HEPES (pH 7.6 with NaOH) at room temperature. The current signals were low-pass-filtered at 1 kHz and no leak subtraction was used. The sampling interval for whole-cell currents ranged from 0.5 to 8 ms.

2.4. Drugs

Nifekalant (Nihon Schering, Osaka, Japan) was prepared as a stock solution (10 mM). Before the experiments, the stock solution was diluted with bath solution to reach the desired final concentration.

2.5. Statistics

All values are presented in terms of means ± S.E. Analysis by Student's *t*-test was performed for paired or unpaired observations. A P value of less than 0.05 was considered significant.

3. Results

3.1. Concentration dependence of HERG channel blockade by nifekalant

The effects of nifekalant on HERG currents elicited by depolarization steps to voltages ranging from −60 to +40 mV are shown in Fig. 1A. Application of nifekalant to the bath solution inhibited the HERG currents in a concentration-dependent manner (Fig. 1B). The concentration–response curve was constructed by plotting the tail currents at −60 mV after a depolarization pulse to +20 mV. The IC_{50} value calculated from the Hill equation was 7.9 μM (Fig. 1C).

3.2. Voltage dependence of HERG channel blockade by nifekalant

The current–voltage relationships at the end of the 3.6-s depolarizing voltage steps were plotted in the absence and presence of 10 μM nifekalant (Fig. 2A). The current–voltage relationship showed a strong inward rectification at potentials positive to −10 mV because of fast C-type inactivation (Smith et al., 1996). Nifekalant at a concentration of 10 μM inhibited the currents at test potentials between −40 and +40 mV. The blockade was enhanced with stronger depolarization between −40 and 0 mV but declined thereafter at more positive potentials up to +40 mV. The tail currents generated after the stimulating pulses increased with voltage and then plateaued at test potentials positive to +10 mV. HERG tail current inhibition was also voltage-dependent. The percent block increased when the conductance of the channels increased steeply. At potentials positive to −10 mV, the percent block of the tail currents plateaued (Fig. 2B).

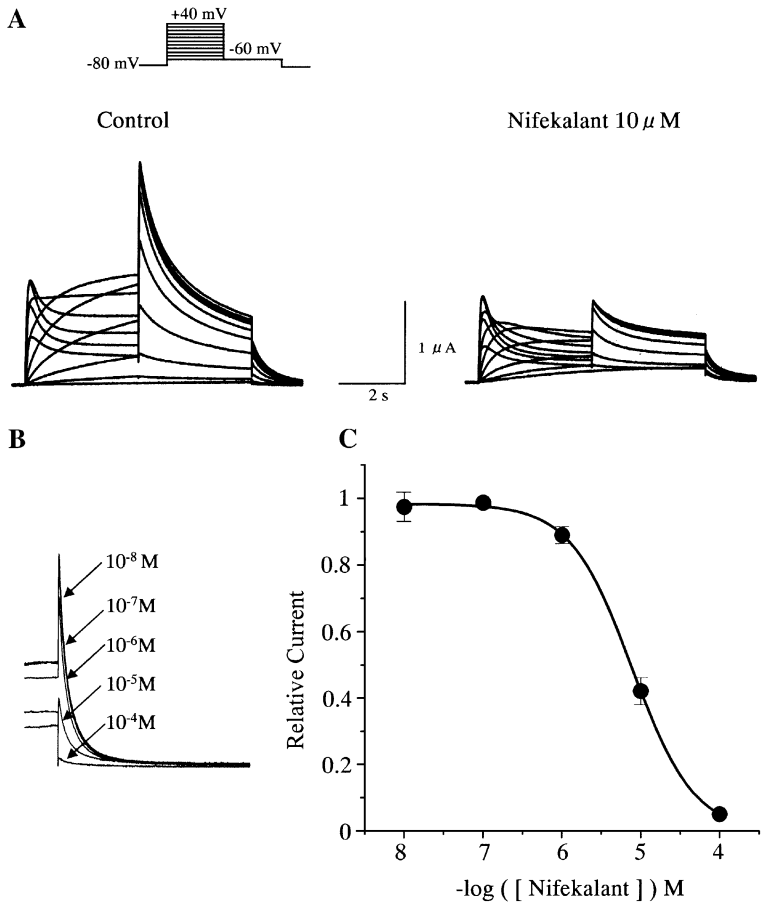

Fig. 1. Effect of nifekalant on HERG channels. (A) Representative traces of HERG channel currents under control conditions (left) and after application of 10 μM nifekalant (right). Currents were recorded by applying depolarizing test pulses from a holding potential of −80 mV to various potentials between −60 and +40 mV in 10-mV increments for 3.6 s, followed by a hyperpolarizing pulse to −60 mV for 3.6 s. (B) Nifekalant inhibited the HERG tail current in a concentration-dependent manner. The tail current was elicited by a 3.6-s depolarizing pulse to +20 mV. (C) Relative tail currents were fitted with a Hill equation, yielding an IC_{50} of 7.9 μM ($n=4$).

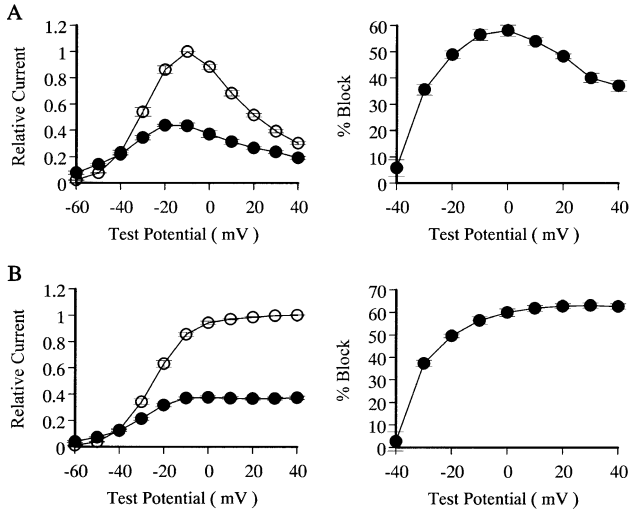

Fig. 2. Block of HERG channels by nifekalant. (A) HERG channel $I-V$ relationships for steady-state currents before (○) and after nifekalant (●), as determined according to the same protocol shown in Fig. 1A ($n=5$). (B) $I-V$ relationships for peak tail currents ($n=5$). The right panels show the percent block of the HERG channels vs. test potentials for the two $I-V$ relationship.

The voltage dependence of HERG channel blockade by nifekalant was assessed with other two different voltage protocols: the fully activated $I-V$ protocol, and the instantaneous $I-V$ protocol. To determine the fully activated $I-V$ relationships, a 750-ms prepulse to +20 mV was applied before each of the repolarizing pulses to test potentials between −120 and +20 mV. The prepulse potential at +20 mV was positive enough to induce full conductance of the HERG channels but also rendered a large number of the channels in the inactivated state. The percent block was almost equal with increasing test potentials from −120 up to −40 mV and declined at more positive potentials within the range where the inward rectification became apparent (Fig. 3A).

We next used instantaneous $I-V$ protocols to evaluate the voltage dependence of HERG channel blockade under conditions by which HERG channel rectification was removed. The channels were first inactivated by clamping the membrane at +40 mV for 1 s, followed by a prepulse to −100 mV for 15 ms. This prepulse was sufficiently long to allow rapid recovery of channels from inactivation but short

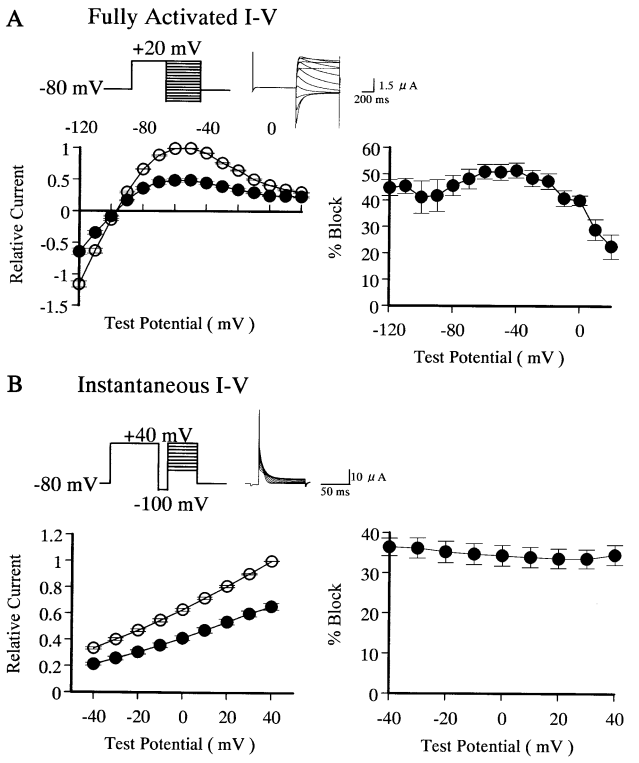

Fig. 3. Voltage dependence of HERG channel blockade by nifekalant, as determined with the fully activated *I–V* protocol (A) and the instantaneous *I–V* protocol (B). (A) In the fully activated *I–V* protocol, each current was obtained by depolarization to +20 mV for 750 ms to reach a steady-state level before repolarization for 750 ms to potentials from +20 to −120 mV. The peak currents before (○) and after nifekalant (●) during repolarization steps were plotted as a function of voltage. (B) With the instantaneous *I–V* protocol, currents were recorded after a 1-s depolarization to +40 mV, followed by a 15-ms hyperpolarizing step to −100 mV to reverse the rapid inactivation and then a 90-ms depolarization to potentials ranging +40 and −40 mV. The right panels show percent block of the HERG channels vs. test potentials for the two voltage protocols.

enough to prevent significant channel deactivation. Following the recovery prepulse, a series of test pulses were delivered to potentials ranging from −40 to +40 mV. The currents recorded were fitted by a single exponential function with extrapolation to the initial point of the test pulse and the amplitude was plotted against the test potential. In this protocol, the proportion of the current blocked by nifekalant did not change significantly between −40 and +40 mV (Fig. 3B).

3.3. Time dependence of HERG channel blockade by nifekalant

The relationship between the level of activation of the HERG channel and the inhibitory effect on the HERG current exerted by nifekalant was assessed from the amplitude of the tail currents at −60 mV after voltage steps to +20 mV of various durations (initial duration 50 ms, increments 50 ms). In the control, the tail current amplitude increased with prolongation of the depolarization pulses. Tail currents reached a steady state when the depolarizing pulse lasted longer than 200 ms. In the presence of 10 μM nifekalant, the tail current amplitude increased in the beginning but decreased as the duration of the voltage step increased. It can be seen from Fig. 4A that the blocking effect of nifekalant was already present after the first of these pulses. After HERG channels were maximally activated, HERG channel blockade continued to increase.

To study recovery from block by nifekalant, a test depolarization was given at variable times after the induction of block by a conditioning pulse protocol. The change

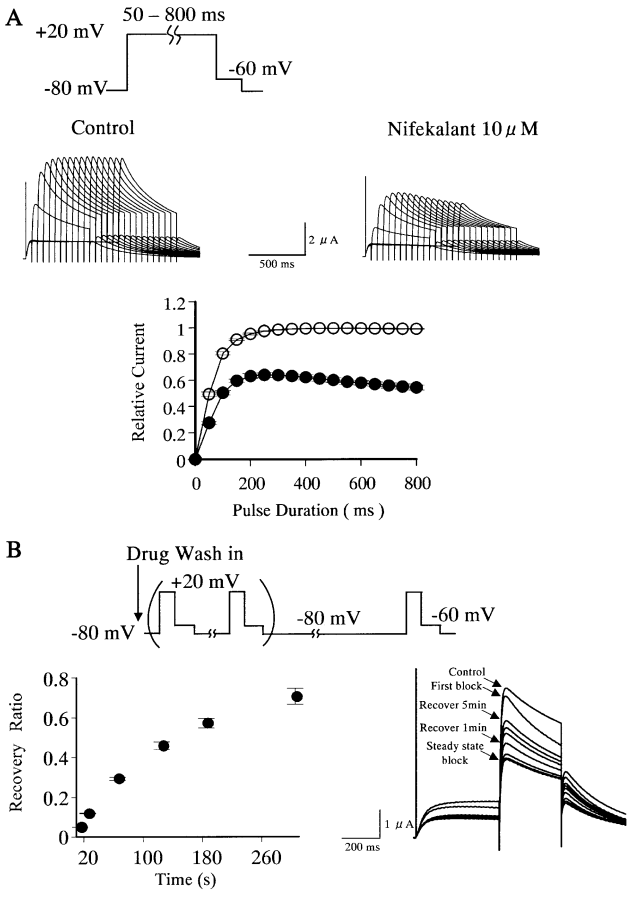

Fig. 4. Time course of blockade of HERG channels by nifekalant. (A) Onset of HERG channel blockade by nifekalant using an envelope tail current protocol. Depolarizing pulses to +20 mV of variable duration (50–800 ms) from a holding potential of −80 mV were applied at 15-s intervals before (○) and after exposure to nifekalant (●). Peak tail currents relative to control maximum tail current were plotted for control and after nifekalant ($n=8$). (B) Recovery from block of HERG channel by nifekalant. Recovery was estimated by applying a holding potential after the induction of block. Tail current amplitude was measured at −60 mV. After measuring the control tail current amplitude for the test pulse, the drug was applied within 2 min, while the membrane was held at −80 mV. After 2 min, the test pulse of 400 ms to +20 mV was applied and the tail current was measured. The test pulse was then repeated at an interval of 5 s until the tail current amplitude declined to a steady state. Recovery was measured at 10, 20, 60, 120, 180 and 300 s ($n=3$).

in the tail current of the test pulse is a measure of recovery from HERG channel blockade by nifekalant. Fig. 4B summarizes the results obtained from three oocytes. After development of the steady-state use-dependent block, the test voltage clamp was applied after 10, 20, 60, 120, 180 and 300 s. The holding potential was −80 mV. As shown in Fig. 4B, the amplitude of the tail current in the presence of 10 μM nifekalant increased with a time constant of 137 s.

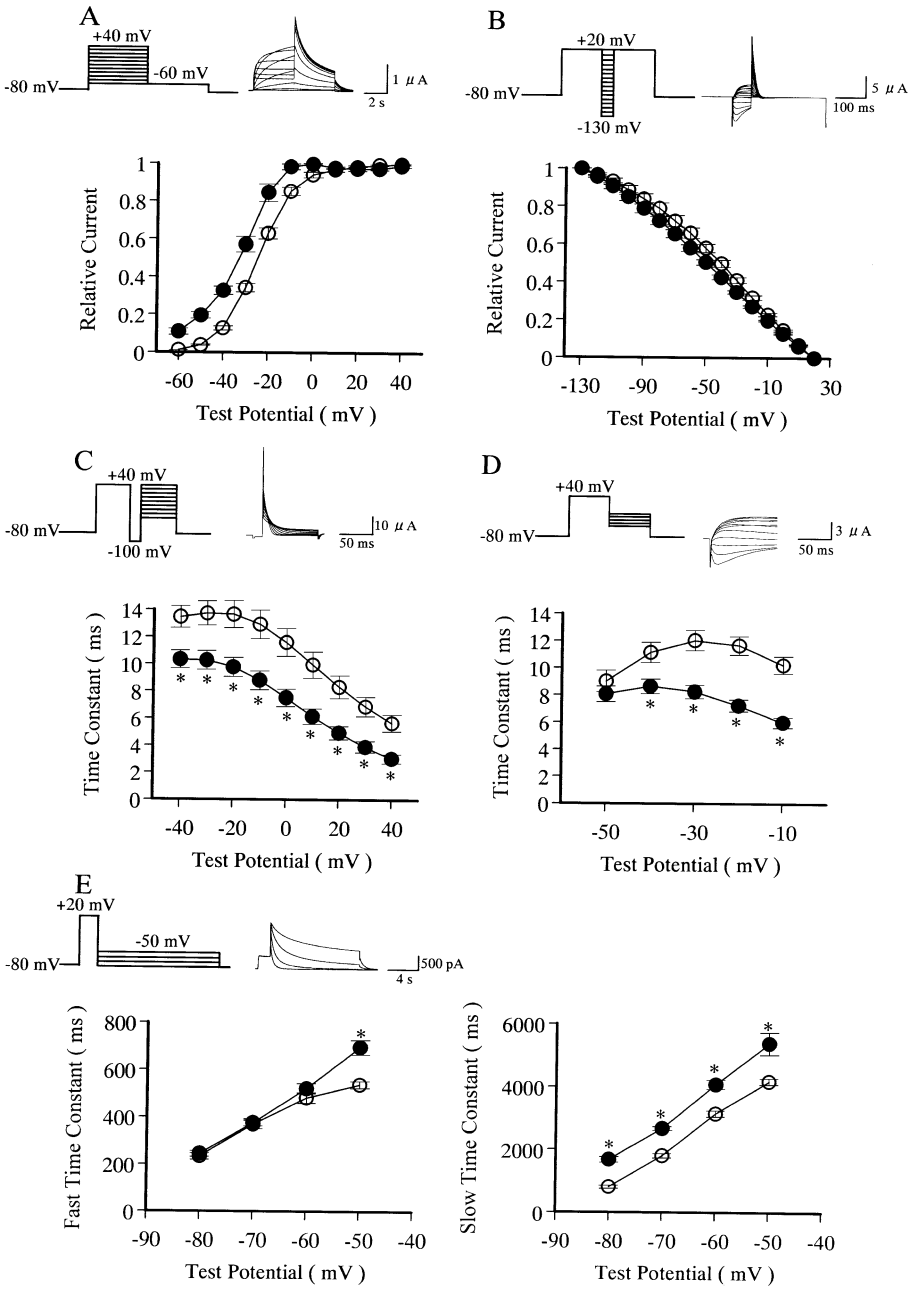

Fig. 5. Effects of nifekalant on HERG channel gating kinetics. (A) Averaged activation curves, as calculated from the normalized peak tail current amplitudes before (○) and after application of 10 μM nifekalant (●) ($n=5$). Smooth curves are best fits of the data to a Boltzmann function. (B) Voltage dependence of steady-state inactivation ($n=8$). Following a 0.9-s step to +20 mV, 60-ms pulses were applied to potentials between −130 and +20 mV, followed by a 240-ms step to +20 mV. Current amplitudes elicited by the second step pulse to +20 mV were plotted as a function of potential of the preceding 60 ms step. (C) Inactivation time constants plotted as a function of membrane potential ($n=8$). Voltage protocol is the same as used in Fig. 3B. (D) Recovery from inactivation ($n=8$). Time constant was determined by fitting a single exponential function to the initial hook preceding slower deactivation of tail currents elicited by stepping to potentials between −50 and −10 mV following a 750-ms depolarization to +40 mV (inset). (E) Deactivation time constants were calculated by best fits to the double exponential function (fast and slow time constant) of the currents elicited by a test pulse between −80 and −50 mV preceded by a 1.6-s prepulse to +20 mV ($n=8$). *$P<0.05$ vs. control.

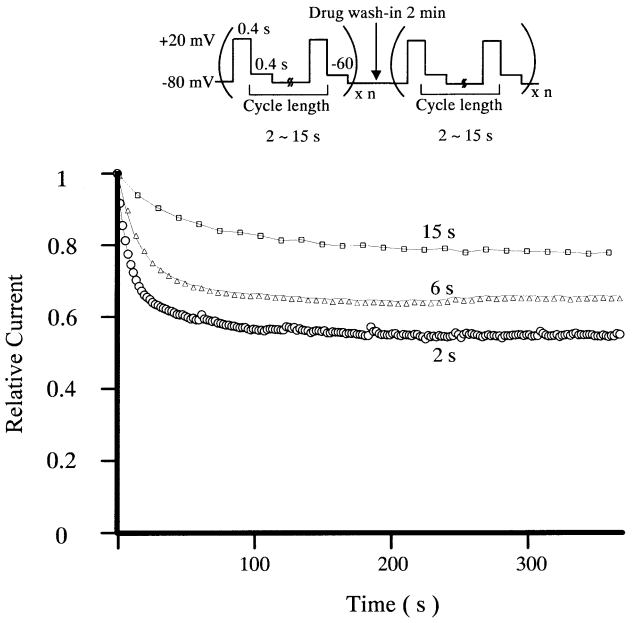

Fig. 6. Use-dependent block of HERG current was tested at pulse intervals of 2 ($n=3$), 6 ($n=3$) and 15 s ($n=3$). The voltage-clamp protocol is illustrated schematically in the inset. Ratios of peak tail current in the presence of nifekalant compared with those of the control were plotted against time after the first pulse.

3.4. Effects of nifekalant on the kinetics of HERG channel currents

Drugs that block ion channels often alter the voltage dependence or kinetics of channel gating. Therefore, we examined the effects of nifekalant on the voltage dependence of activation and rectification and on the kinetics of inactivation and deactivation. The activation curves were constructed by normalizing the tail currents recorded with the protocol used in Fig. 1A. The normalized data were plotted against the test pulse potentials and fitted to the Boltzmann function. As shown in Fig. 5A, nifekalant altered the activation properties: the $V_{1/2}$ values (the half-maximal activation voltage) and the slope factor (k) were -24.7 ± 0.9 and 8.2 ± 0.2 mV before and -31.0 ± 1.1 and 6.8 ± 0.4 mV after nifekalant, respectively (Fig. 5A).

The inactivation characteristics were also affected by nifekalant (Fig. 5B). To construct the inactivation curves, the voltage protocol shown in the inset of Fig. 5B was used: a 900-ms depolarizing pulse to +20 mV to inactivate the HERG channels, followed by varying repolarizing pulses to potentials between −130 and +20 mV for a short period to allow full recovery of channels from inactivation at more negative potentials and rapid inactivation at +20 mV. Nifekalant produced a negative shift of the inactivation curve.

The inactivation process was analyzed by fitting the currents elicited by the voltage protocol described for the voltage-dependent inactivation (Fig. 5C). A 1-s depolarization to +40 mV was followed by a 15-ms hyperpolarizing step to −100 mV to relieve the rapid inactivation. A second pulse to potentials between −40 and +40 mV was then used to elicit large currents that underwent rapid re-inactivation. The time constant of inactivation was determined by fitting a single exponential function to these currents. Fig. 5C shows that inactivation was accelerated in the presence of 10 μM nifekalant at all potentials ($\tau = 13.4 \pm 0.8$ ms before and 10.3 ± 0.7 ms after nifekalant at −40 mV, $P<0.05$, $n=8$).

Recovery from inactivation was determined by fitting a single exponential function to the initial hook preceding the slower deactivation of tail currents at potentials between −50 and −10 mV. Nifekalant decreased the time constant of recovery from inactivation between −40 and −10 mV ($\tau = 11.1 \pm 0.8$ ms before and 8.6 ± 0.5 ms after nifekalant at −40 mV, $P<0.05$, $n=8$) (Fig. 5D). We studied the deactivation of tail currents produced by a 1.6-s pulse to +20 mV followed by a 12-s repolarization between −80 and −50 mV. Nifekalant significantly delayed the slow component of deactivation but did not affect the fast component of deactivation (Fig. 5E).

3.5. Frequency dependence of HERG channel blockade by nifekalant

We examined the use dependence (frequency dependence) of inhibition of the HERG current by nifekalant

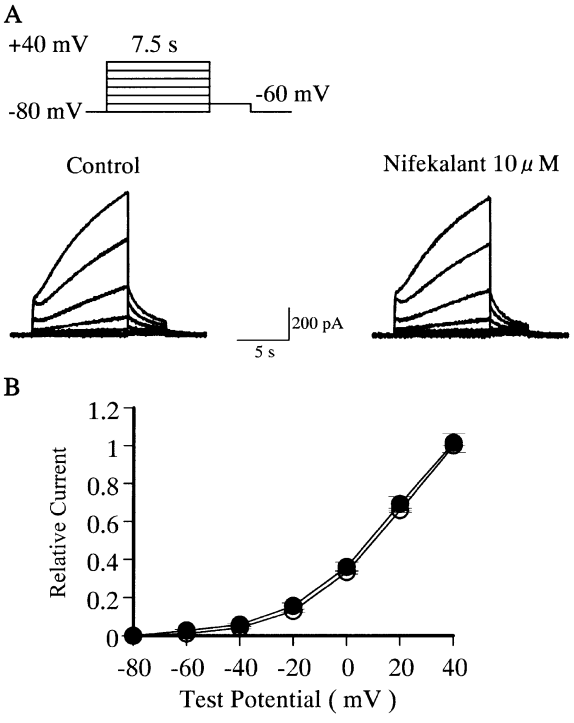

Fig. 7. Effect of nifekalant on minK currents. (A) Representative traces of minK currents under control conditions (○) and in the presence of 10 μM nifekalant (●). Currents were recorded by applying depolarizing test pulses from a holding potential of −80 mV to various potentials between −80 and +40 mV in 20-mV increments for 7.5 s, followed by a hyperpolarizing pulse to −60 mV for 2.5 s. (B) I–V relationship for minK currents measured at the end of the 7.5-s depolarization step ($n=7$).

(Fig. 6). The HERG current was elicited by 0.4-s voltage steps from −80 to +20 mV, followed by a 0.4-s step to −60 mV to record outward tail currents at intervals of 2, 6 and 15 s. The level of steady-state block is a measure of the use dependence of block. Block was use-dependent, with stronger block at higher frequencies than at lower frequencies.

3.6. Effects of nifekalant on minK channel current

We examined the effects of nifekalant on the K^+ currents in oocytes expressing minK channels (Fig. 7). The oocytes expressing minK channels were voltage-clamped at −80 mV and voltage pulses of 7.5-s duration were applied to potentials between −80 and +40 mV in 20-mV increments. The tail currents were recorded on repolarization to −60 mV. The minK currents were unaffected by the application of nifekalant (10 and 30 μM) to the bath solution.

4. Discussion

In experiments with cardiac cells from rabbits and guinea pigs, nifekalant was shown to decrease I_K, which is probably I_{Kr} but not I_{Ks} (Nakaya et al., 1993; Cheng et al., 1996; Nakaya and Uemura, 1998). In the present study, we confirmed that nifekalant effectively blocks HERG channels expressed in *Xenopus* oocytes with an IC_{50} of 7.9 μM. In contrast, nifekalant failed to inhibit minK currents. These findings indicate that nifekalant selectively blocks the rapidly activating component of the delayed rectifier potassium current (I_{Kr}) in human cardiomyocytes.

Inhibition of HERG channels by nifekalant showed voltage dependence. Nifekalant inhibited the HERG currents more effectively when the membrane was depolarized. Nifekalant inhibited HERG currents ~5% at a depolarizing potential of −40 mV and ~60% at 0 mV. In the fully activated $I–V$ protocol (Fig. 3A), where the full conductance of the HERG channels was induced, nifekalant inhibited HERG currents ~50% even at a hyperpolarizing potential of −120 mV. These findings suggest that nifekalant binds to HERG channels that are in the open state.

The magnitude of HERG current inhibition by nifekalant decreased at more depolarizing potentials, where the fraction of the inactivated HERG channels increased. HERG current inhibition by the drug was almost similar at all depolarizing potentials when we recorded the current using the instantaneous $I–V$ protocol (Fig. 3B), which attenuated channel inactivation (Smith et al., 1996). These results suggest that nifekalant has a lower binding affinity for the inactivate state than for the open state.

Envelope of the tail current protocol showed that the blocking effect of HERG channels by nifekalant was already present when the first depolarizing pulse was applied. Nifekalant might have access to HERG channels immediately after HERG channels become open. Another possibility is that nifekalant also may have affinity for the close state and produce tonic block.

The time course of recovery of HERG channels from blockade by nifekalant at −80 mV was slow, with a recovery time constant of 137 s. In rabbit ventricular myocytes, however, recovery from the blockade of I_K by nifekalant was reported to be very rapid at −75 mV (time constant 577 ms) (Cheng et al., 1996). This discrepancy might arise from differences in experimental protocol used for determination of the recovery time constant in these studies. Cheng et al. applied one conditioning pulse to +10 mV from a holding potential of −50 mV to get a steady-state block. In our study, we applied conditioning pulses to +20 mV from a holding potential of −80 mV at a frequency of 0.2 Hz for 4 min to obtain a steady-state block. Another possibility is that native cardiac myocytes may have endogenous channel subunits and/or regulatory molecules that can affect the recovery from blockade (Abbott et al., 1999). Homomultimer HERG channels expressed in heterologous expression systems may have a longer recovery time than that of native I_{Kr} channels in cardiac myocytes.

The onset of HERG blockade by nifekalant was very rapid but recovery from the blockade was very slow. A slow recovery from blockade causes use-dependent block. HERG blockade continued to increase after HERG channels were maximally activated in the envelope of the tail current protocol. The envelope test protocol was applied at a pulse interval of 15 s, but this duration was not long enough for nifekalant to dissociate from HERG channels. The blockade by nifekalant might become cumulative even after HERG channels are maximally activated.

The voltage of half-maximal activation ($V_{1/2}$) was shifted to more negative potentials. Nifekalant augmented the HERG tail currents at membrane potentials negative to −40 mV (Fig. 2A). The increase in the HERG current may be ascribed to a partial agonistic effect of nifekalant. A similar phenomenon has been reported with other class III drugs such as almokalant (Carmeliet, 1993) or azimilide (Jiang et al., 1999). Nifekalant inhibited the HERG currents more effectively when the membrane was depolarized. Therefore, when the current amplitude was normalized to the maximum value in the presence of nifekalant, the proportion of the current amplitude at negative potentials apparently increased relative to that at positive potentials. This might be responsible for the negative shift of the activation curve.

Nifekalant also shifted the inactivation curve in a negative direction. Both the time constant of onset of inactivation and the time constant of recovery from inactivation were accelerated in the presence of nifekalant. Other class III antiarrhythmic drugs are suggested to bind near the pore helix (Mitcheson et al., 2000). The binding site for nifekalant on the channel may be around the pore helix that controls channel inactivation. The binding of nifekalant

may lead to acceleration of the transition rate between the open and inactive state or alter the voltage dependence of channel inactivation. Nifekalant increased τ_{slow} of deactivation, probably by preventing the activation gate from closing due to slow dissociation of the drug during channel deactivation.

Ideally, K^+ channel blockade by class III antiarrhythmic drugs should be more marked at faster heart rates, but actually, the prolongation of the action potential duration by many class III antiarrhythmic drugs is exaggerated at slower heart rates. Excessive prolongation of the action potential duration with these drugs under physiological heart rates has been implicated as a cause of torsades de pointes (Roden and Hoffman, 1985). This is a common unfavorable feature of new class III antiarrhythmic drugs. It has been reported that, in isolated rabbit ventricular cells, nifekalant produce a bell-shaped frequency–response curve: the maximum prolongation of action potential duration was observed at 1.0-Hz stimulation and the action potential duration-prolonging effect was attenuated at lower (up to 0.1 Hz) and higher stimulus frequencies (up to 3.3 Hz) (Cheng et al., 1996). In this respect, nifekalant differs from other conventional and newer class III drugs, such as sotalol, E-4031, dofetilide, UK-66914 and almokalant, that show reverse frequency-dependent block. In our study, nifekalant inhibited HERG currents in a frequency-dependent manner. Steady-state inhibition under 0.5-Hz stimulation (interval 2 s) was greater than that at 0.17-Hz stimulation (interval 6 s). Although we could not apply higher stimulus frequencies in our protocol, our results under low stimulus frequency conditions (between 0.07 and 0.5 Hz) are consistent with results obtained with rabbit ventricular cells (Cheng et al., 1996). It has been suggested that the mechanism responsible for the reverse use dependence of action potential duration prolongation is not caused by the frequency dependence of antiarrhythmic drugs in inhibiting a specific current. Other currents, such as the inward rectifier current (I_{K1}), the Ca^{2+} current, the Na^+–K^+ pump current, the Na^+–Ca^{2+} exchanger current, and the slowly inactivating Na^+ current, also contribute to the frequency dependence of action potential duration prolongation (Williams et al., 1999; Li et al., 1999). In this study, nifekalant showed a frequency-dependent inhibition of HERG channels. However, it has been reported that nifekalant fails to prolong the action potential duration in a frequency-dependent manner in native cardiomyocytes (Nakaya et al., 1993; Cheng et al., 1996). Frequency-dependent activation of I_{Ks} might mask the inhibitory effect of nifekalant on I_{Kr} at rapid stimulation rates since nifekalant hardly affected the minK current in this study.

Nifekalant inhibits HERG channels in a voltage-dependent as well as frequency-dependent manner because of its high affinity for the open state of HERG channels. The potent inhibition of HERG channels by nifekalant underlies its remarkable effectiveness against malignant ventricular tachyarrhythmias in clinical settings.

Acknowledgements

We are grateful to M. Tamagawa for technical assistance and I. Sakashita for secretarial assistance. This work was supported in part by a Grant-in-Aid from the Ministry of Education, Science, Sports and Culture of Japan and K. Watanabe Research Fund.

References

Abbott, G.W., Sesti, F., Splawski, I., Buck, M.E., Lehmann, M.H., Timothy, K.W., Keating, M.T., Goldstein, S.A., 1999. MiRP1 forms I_{Kr} potassium channels with HERG and is associated with cardiac arrhythmia. Cell 97, 175–187.

Carmeliet, E., 1993. Use-dependent block and use-dependent unblock of the delayed rectifier K^+ current by almokalant in rabbit ventricular myocytes. Circ. Res. 73, 857–868.

Cheng, J., Kamiya, K., Kodama, I., Toyama, J., 1996. Differential effects of MS-551 and E-4031 on action potentials and the delayed rectifier K^+ current in rabbit ventricular myocytes. Cardiovasc. Res. 31, 963–974.

Friedrichs, G.S., Chi, L., Black, S.C., Manley, P.J., Lucchesi, B.R., 1994. Antiarrhythmic agent, MS-551, protects against pinacidil + hypoxia-induced ventricular fibrillation in Langendorff-perfused rabbit isolated heart. J. Cardiovasc. Pharmacol. 23, 120–126.

Friedrichs, G.S., Chi, L., Gralinski, M.R., Black, S.C., Balser, G.C., Mu, D.X., Pewitt, S.R., Johnson, C.R., Lucchesi, B.R., 1995. MS-551 protects against ventricular fibrillation in a chronic canine model of sudden cardiac death. J. Cardiovasc. Pharmacol. 25, 314–323.

Hashimoto, K., Haruno, A., Hirasawa, A., Awaji, T., Xue, Y., Wu, Z., 1995. Effects of the new class III antiarrhythmic drug MS-551 and D-sotalol on canine coronary ligation-reperfusion ventricular arrhythmias. Jpn. J. Pharmacol. 68, 1–9.

Hondeghem, L.M., Snyders, D.J., 1990. Class III antiarrhythmic agents have a lot of potential but a long way to go. Reduced effectiveness and dangers of reverse use dependence. Circulation 81, 686–690.

Jiang, M., Dun, W., Fan, J.S., Tseng, G.N., 1999. Use-dependent 'agonist' effect of azimilide on the HERG channel. J. Pharmacol. Exp. Ther. 291, 1324–1336.

Kamiya, J., Ishii, M., Katakami, T., 1992. Antiarrhythmic effects of MS-551, a new class III antiarrhythmic agent, on canine models of ventricular arrhythmia. Jpn. J. Pharmacol. 58, 107–115.

Koizumi, T., Komiyama, N., Komuro, I., Tanigawa, T., Iwase, T., Ishiwata, S., Nishiyama, S., Momomura, S., 2001. Efficacy of nifekalant hydrochloride on the treatment of life-threatening ventricular tachyarrhythmias during reperfusion for acute myocardial infarction. Cardiovasc. Drugs Ther. 15, 363–365.

Kondoh, K., Hashimoto, H., Nishiyama, H., Umemura, K., Ozaki, T., Uematsu, T., Nakashima, M., 1994. Effects of MS-551, a new class III antiarrhythmic drug, on programmed stimulation-induced ventricular arrhythmias, electrophysiology, and hemodynamics in a canine myocardial infarction model. J. Cardiovasc. Pharmacol. 23, 674–680.

Li, G.R., Yang, B.F., Feng, J.L., Bosch, R.F., Carrier, M., Nattel, S., 1999. Transmembrane I_{Ca} contributes to rate-dependent changes of action potentials in human ventricular myocytes. Am. J. Physiol. 276, H98–H106.

Martin, D.K., Nakaya, Y., Wyse, K.R., Bursill, J.A., West, P.D., Campbell, T.J., 1995. Inhibition of ATP-sensitive potassium channels in cardiac myocytes by the novel class III antiarrhythmic agent MS-551. Pharmacol. Toxicol. 77, 65–70.

Mason, J.W., 1993. A comparison of seven antiarrhythmic drugs in patients with ventricular tachyarrhythmias. N. Engl. J. Med. 329, 452–458.

Mitcheson, J.S., Chen, J., Lin, M., Culberson, C., Sanguinetti, M.C., 2000. A structural basis for drug-induced long QT syndrome. Proc. Natl. Acad. Sci. U. S. A. 22, 12329–12333.

Mori, K., Hara, Y., Saito, T., Masuda, Y., Nakaya, H., 1995. Anticholinergic effects of class III antiarrhythmic drugs in guinea pig atrial cells. Different molecular mechanisms. Circulation 91, 2834–2843.

Murakawa, Y., Yamashita, T., Kanese, Y., Omata, M., 1997. Can a class III antiarrhythmic drug improve electrical defibrillation efficacy during ventricular fibrillation? J. Am. Coll. Cardiol. 29, 688–692.

Nakaya, H., Uemura, H., 1998. Electropharmacology of nifekalant, a new class III antiarrhythmic drug. Cardiovasc. Drug Rev. 16, 133–144.

Nakaya, H., Tohse, N., Takeda, Y., Kanno, M., 1993. Effects of MS-551, a new class III antiarrhythmic drug, on action potential and membrane currents in rabbit ventricular myocytes. Br. J. Pharmacol. 109, 157–163.

Roden, D.M., Hoffman, B.F., 1985. Action potential prolongation and induction of abnormal automaticity by low quinidine concentrations in canine Purkinje fibers. Relationship to potassium and cycle length. Circ. Res. 56, 857–867.

Sato, R., Koumi, S., Hisatome, I., Takai, H., Aida, Y., Oyaizu, M., Karasaki, S., Mashiba, H., Katori, R., 1995. A new class III antiarrhythmic drug, MS-551, blocks the inward rectifier potassium channel in isolated guinea pig ventricular myocytes. J. Pharmacol. Exp. Ther. 274, 469–474.

Smith, P.L., Baukrowitz, T., Yellen, G., 1996. The inward rectification mechanism of the HERG cardiac potassium channel. Nature 379, 767–768.

Takenaka, K., Yasuda, S., Miyazaki, S., Kurita, T., Sutani, Y., Morii, I., Daikoku, S., Kamakura, S., Nonogi, H., 2001. Initial experience with nifekalant hydrochloride (MS-551), a novel class III antiarrhythmic agent, in patients with acute extensive infarction and severe ventricular dysfunction. Jpn. Circ. J. 65, 60–62.

Trudeau, M.C., Warmke, J.W., Ganetzky, B., Robertson, G.A., 1995. HERG, a human inward rectifier in the voltage-gated potassium channel family. Science 269, 92–95.

Waldo, A.L., Cann, A.J., Deruyter, H., Freidman, P.L., Macneil, D.J., Pitt, B., Pratt, C.M., Rodda, B.E., Schwartz, P.J., 1995. Survival with oral D-sotalol in patients with left ventricular dysfunction after myocardial infarction: rationale, design, and methods (the SWORD trial). Am. J. Cardiol. 75, 1023–1027.

Williams, B.A., Dickenson, D.R., Beatch, G.N., 1999. Kinetics of rate-dependent shortening of action potential duration in guinea-pig ventricle: effects of I_{K1} and I_{Kr} blockade. Br. J. Pharmacol. 126, 1426–1436.